PHYSICAL REVIEW D **90,** 096010 (2014)

Arbitrary mass Majorana neutrinos in neutrinoless double beta decay

Amand Faessler,[1] Marcela González,[2] Sergey Kovalenko,[2] and Fedor Šimkovic[3,4,5]

[1]*Institute für Theoretische Physik der Univesität Tübingen, Auf der Morgenstelle 14, D-72076 Tübingen, Germany*

[2]*Universidad Técnica Federico Santa María, Centro-Científico-Tecnológico de Valparaíso, Casilla 110-V Valparaíso, Chile*

[3]*Bogoliubov Laboratory of Theoretical Physics, JINR 141980 Dubna, Russia*

[4]*Department of Nuclear Physics and Biophysics, Comenius University, Mlynská dolina F1, SK-842 48 Bratislava, Slovakia*

[5]*Czech Technical University in Prague, 128-00 Prague, Czech Republic*

(Received 20 October 2014; published 21 November 2014)

We revisit the mechanism of neutrinoless double beta ($0\nu\beta\beta$) decay mediated by the exchange with the heavy Majorana neutrino N of arbitrary mass m_N, slightly mixed $\sim U_{eN}$ with the electron neutrino ν_e. By assuming the dominance of this mechanism, we update the well-known $0\nu\beta\beta$-decay exclusion plot in the $m_N - U_{eN}$ plane taking into account recent progress in the calculation of nuclear matrix elements within quasiparticle random phase approximation and improved experimental bounds on the $0\nu\beta\beta$-decay half-life of ^{76}Ge and ^{136}Xe. We also consider the known formula approximating the m_N dependence of the $0\nu\beta\beta$-decay nuclear matrix element in a simple explicit form. We analyze its accuracy and specify the corresponding parameters, allowing one to easily calculate the $0\nu\beta\beta$-decay half-life for arbitrary m_N for all the experimentally interesting isotopes without resorting to real nuclear structure calculations.

DOI: 10.1103/PhysRevD.90.096010 PACS numbers: 11.30.Fs, 14.60.Pq, 14.60.St, 23.40.-s

I. INTRODUCTION

After the triumph of the neutrino oscillation and the LHC experiments in discovering two long-awaited key elements of nature, neutrino mass and mixing as well as the Higgs boson, the next breakthrough of comparable magnitude may happen in neutrinoless double beta ($0\nu\beta\beta$)-decay searches. This hope is fed from both the theoretical and experimental sides. Lepton number violation (LNV) is forbidden in the Standard Model, and therefore observation of any LNV process would have a profound impact on particle physics and cosmology. In particular, it would prove that neutrinos are Majorana particles [1,2], indicate the existence of a new high-energy LNV scale and related new physics [3], and provide a basis for a solution of the problem of matter-antimatter asymmetry of the Universe via leptogenesis [4]. Among the LNV processes, $0\nu\beta\beta$ decay is widely recognized as the most promising candidate for experimental searches. Another possible probe of LNV, which, as it has been recently realized, could be competitive or complementary to $0\nu\beta\beta$ decay, is the like-sign dilepton [5,6] searches at the LHC [7–11]. However, this option still requires detailed studies to clarify its status. On the experimental side of the $0\nu\beta\beta$ decay, one expects a significant progress in the sensitivities of near-future experiments, stimulating the hopes for observation of this LNV process (for a recent review, see e.g., Ref. [12]).

The theory of $0\nu\beta\beta$ decay deals with three energy scales associated with rather different physics, namely, (1) the LNV scale and underlying quark-level mechanisms of $0\nu\beta\beta$ decay, (2) hadronic scale $\sim$1 GeV and QCD effects including nucleon form factors, and (3) nuclear scale $p_F \sim (100–200)$ MeV and nuclear structure arrangement (p_F is the nucleon Fermi momentum in a nucleus). In the literature, all these three structure levels have been addressed from different perspectives (see e.g., Refs. [12–14]).

In the present paper, we revisit the mechanisms of $0\nu\beta\beta$ decay mediated by Majorana neutrino N exchange with an arbitrary mass m_N [15]. Our goal is to update and extend the analysis [16] of the case with several mass eigenstates N dominated by “sterile” neutrinos ν_s and with an admixture U_{eN} of the active flavor ν_e. Massive neutrinos N have been considered in the literature in divers contexts (see e.g., Ref. [17]) with the masses m_N ranging from the eV to the Planck scale. Their phenomenology has been actively studied from various perspectives including their contribution to particle decays and production in collider experiments (for a recent review, see e.g., Refs. [18,19]). The corresponding searches for N have been carried out in various experiments [20]. An update of the previous analysis of Ref. [16] is needed because of the recent progress in the calculation of the double beta-decay nuclear matrix elements (NMEs), which includes constraints on the nuclear Hamiltonian from the two-neutrino double beta-decay half-life [21,22], a self-consistent description of the two-nucleon short-range correlations [23], and the restoration of isospin symmetry [24]. Our framework is given by the quasiparticle random phase approximation (QRPA). Recently, the analysis of massive sterile neutrinos in $0\nu\beta\beta$ decay within another approach, the interacting shell model, was carried out in Ref. [25]. There has also been significant progress in $0\nu\beta\beta$-decay experiments [12], especially for ^{76}Ge [26] and ^{136}Xe [27] isotopes, which allows improvements of the previous limits in the neutrino sector.

The paper is organized as follows. In the next section, Sec. II, we set up the formalism underlying our analysis of the Majorana exchange mechanism of $0\nu\beta\beta$ decay. Then, we calculate the corresponding NMEs. Section III deals with an approximate formula for the NMEs explicitly representing their dependence on m_N for arbitrary values of this parameter. In Sec. IV, we extract the $0\nu\beta\beta$-decay limits in the parameter plane $m_N - |U_{eN}|^2$ and compare them with other existing limits [20].

II. FORMALISM

We assume that, in addition to the three conventional light neutrinos, there exist other Majorana neutrino mass eigenstates N of an arbitrary mass m_N, dominated by the sterile neutrino species ν_s and with some admixture of the active neutrino weak eigenstates, $\nu_{e,\mu,\tau}$, as

$$N = \sum_{\alpha=s,e,\mu,\tau} U_{N\alpha}\nu_\alpha. \tag{1}$$

The phenomenology of the intermediate mass sterile neutrinos N in various LNV processes has been actively studied in the literature (for a recent review, see e.g., Refs. [18,19]), and limits in the $|U_{\alpha N}|^2 - m_N$-plane have been derived. It has been shown that $0\nu\beta\beta$-decay limits for $|U_{eN}|^2 - m_N$ are the most stringent in comparison with the limits from the other LNV processes except for a narrow region of this parametric plane [16,19,28].

We study the possible contributions of these N neutrino states to $0\nu\beta\beta$ decay via a nonzero admixture of a ν_e weak eigenstate. From nonobservation of this LNV process, we update the stringent limits on the $\nu_N - \nu_e$ mixing matrix element U_{eN} in a wide region of the values of m_N. We compare these limits with the corresponding limits derived from the searches for some other LNV processes. We also discuss typical uncertainties of our calculations originating from the models of nucleon and nuclear structure.

The contribution of Majorana neutrino state, N, to the $0\nu\beta\beta$-decay amplitude is described by the standard neutrino exchange diagram between the two β-decaying neutrons. Assuming the dominance of this LNV mechanism, the $0\nu\beta\beta$-decay half-life for a transition to the ground state of the final nucleus takes the form

$$[T^{0\nu}_{1/2}]^{-1} = G^{0\nu} g_A^4 \left|\sum_N (U^2_{eN} m_N) m_p M'^{0\nu}(m_N, g_N^{\rm eff})\right|^2. \tag{2}$$

The proton mass is denoted by m_p. The phase-space factor $G^{0\nu}$ is tabulated for various $0\nu\beta\beta$-decaying nuclei in Ref. [29]. In the above formula, g_A and $g_A^{\rm eff}$ stand for the standard and "quenched" values of the nucleon axial-vector coupling constant, respectively. Their meanings will be discussed in what follows. The nuclear matrix element in question, $M'^{0\nu}$, is given by

$$\begin{aligned} M'^{0\nu}&(m_N, g_A^{\rm eff}) \\ &= \frac{1}{m_p m_e}\frac{R}{2\pi^2 g_A^2}\sum_n \int d^3x d^3y d^3p \\ &\quad\times e^{ip\cdot(\mathbf{x}-\mathbf{y})}\frac{\langle 0_F^+|J^{\mu\dagger}(\mathbf{x})|n\rangle\langle n|J^\dagger_\mu(\mathbf{y})|0_I^+\rangle}{\sqrt{p^2+m_N^2}\left(\sqrt{p^2+m_N^2}+E_n-\frac{E_I-E_F}{2}\right)}. \end{aligned} \tag{3}$$

Here, R and m_e are the nuclear radius and the mass of the electron, respectively. We use as usual $R = r_0 A^{1/3}$ with $r_0 = 1.2$ fm. Initial and final nuclear ground states with energies E_I and E_F are denoted by $|0_I^+\rangle$ and $|0_F^+\rangle$, respectively. The summation runs over intermediate nuclear states $|n\rangle$ with energies E_n. The dependence on $g_A^{\rm eff}$ enters to $M'^{0\nu}$ through the weak one-body nuclear charged current $J^\dagger_\mu$, given by

$$\begin{aligned} J^{0\dagger}(\mathbf{r}) &= \sum_{i=1}^{A}\tau_i^+ J_i^0\delta(\mathbf{r}-\mathbf{r}_i), \\ \mathbf{J}^\dagger(\mathbf{r}) &= \sum_{i=1}^{A}\mathbf{J}_i\tau_i^+\delta(\mathbf{r}-\mathbf{r}_i), \end{aligned} \tag{4}$$

where the sum is taken over the total number A of nucleons in a nucleus. The operators with subscript i act only on the ith nucleon. The isospin rising operator τ^+ converts the neutron to a proton. The coordinates of beta-decaying nucleons are denoted by $\mathbf{r}_i$. In the leading order of nonrelativistic approximation, one has

$$\begin{aligned} J^{0\dagger} &= g_V(p^2), \\ \mathbf{J}^\dagger &= -g_A(p^2)\boldsymbol{\sigma} + g_P(p^2)\frac{\mathbf{p}(\boldsymbol{\sigma}\cdot\mathbf{p})}{2m} \\ &\quad - i(g_V(p^2)+g_M(p^2))\frac{\boldsymbol{\sigma}\times\mathbf{p}}{2m}. \end{aligned} \tag{5}$$

Here, $\mathbf{p} = \mathbf{p}_n - \mathbf{p}_p$, with $\mathbf{p}_n$ and $\mathbf{p}_p$ being the initial neutron and the final proton 3-momenta, respectively. For the nucleon electroweak form factors, we use the standard parametrization,

$$\begin{aligned} g_V(p^2) &= \left(1+\frac{p^2}{M_V^2}\right)^{-2}, \\ g_A(p^2) &= g_A^{\rm eff}\left(1+\frac{p^2}{M_A^2}\right)^{-2}, \\ g_M(p^2) &= (\mu_p-\mu_n)g_V(p^2), \\ g_P(p^2) &= 2m_p g_A(p^2)(p^2+m_\pi^2)^{-1}, \end{aligned} \tag{6}$$

where $(\mu_p-\mu_n) = 3.70$, $M_V = 850$ MeV, $M_A = 1086$ MeV, and m_π is the pion mass. For the induced pseudoscalar form factor $g_P(p^2)$, the standard Goldberger–Treiman relation is assumed.

The value of the nucleon axial-vector coupling constant in vacuum is $g_A = 1.269$. In the nuclear medium, this constant is expected to be renormalized to some smaller, the so-called quenched, value $g_A^{\rm eff}$ [30]. This is motivated, in particular, by the fact that the calculated values of the strength of the Gamow–Teller β-decay transitions to individual final states are significantly larger than the experimentally measured ones. Theoretically, the Gamow–Teller strength is a monotonically increasing function of g_A. Therefore, this discrepancy with experiment can be rectified by a proper adjustment of g_A to some smaller quenched value $g_A^{\rm eff}$. It was shown in Refs. [21,21], that this value is compatible with the quark axial-vector coupling $g^{\rm eft} = g_A^{\rm quark} = 1$. In some recent works, $g_A^{\rm eff} < 1$ has been advocated [31,32]. In our opinion, this sort of strong quenching still requires a more firm justification. Therefore, in our analysis, we consider the following two options:

$$g_A^{\rm eff} = g_A = 1.269 \quad [20], \tag{7}$$

$$g_A^{\rm eff} = g_A^{\rm quark} = 1 \quad [21, 21]. \tag{8}$$

We calculated the NME defined in Eq. (3) within the QRPA with partial restoration of isospin symmetry [24]. Two different types of NN potentials charge-dependent Bonn (CD–Bonn) and Argonne as well as unquenched and quenched values of the nucleon axial-vector coupling in Eqs. (7) and (8) were considered. The results for the particular cases of ^{76}Ge and ^{136}Xe we show in Fig. 1. The widths of the blue bands illustrate the typical uncertainties of our approach related to the choice of the NN potential and the value of $g_A^{\rm eff}$.

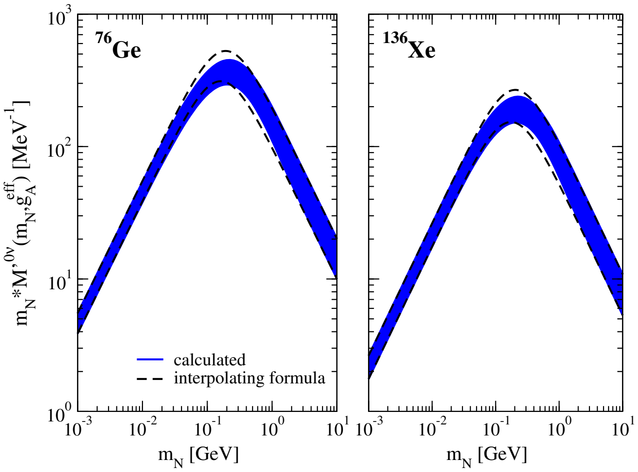

FIG. 1 (color online). The product $m_N M^{0\nu}(m_N)$ vs mass of heavy neutrino m_N for ^{76}Ge and ^{136}Xe within QRPA with partial restoration of isospin symmetry [24]. The filled blue area represents the uncertainty associated with the choice of the NN potential (CD–Bonn and Argonne potentials) and the value of the nucleon axial-vector constant ($g_A^{\rm eff} = 1.0$ and 1.269). The dashed lines and the area between them correspond to results obtained with the approximate formula in Eq. (13).

III. “INTERPOLATING” FORMULA

We have also carried out the calculations of the NME in Eq. (3) for the two conventional limiting cases: the light $m_N \ll p_F$ and the heavy $m_N \gg p_F$ Majorana neutrino exchange mechanisms, where $p_F \sim 200$ MeV is the characteristic momentum transferred via the virtual neutrino, which is of the order of the mean nucleon momentum of Fermi motion in a nucleus. For these limiting cases, the half-life formula (2) is reduced to

$$[T_{1/2}^{0\nu}]^{-1} = G^{0\nu} g_A^4 \begin{cases} \left|\frac{\langle m_\nu\rangle}{m_e}\right|^2 |M_\nu'^{0\nu}(g_A^{\rm eff})|^2, & \text{for } m_N \ll p_F, \\ \left|\left\langle \frac{1}{m_N}\right\rangle m_p\right|^2 |M_N'^{0\nu}(g_A^{\rm eff})|^2, & \text{for } m_N \gg p_F, \end{cases} \tag{9}$$

with

$$\langle m_\nu\rangle = \sum_N U_{eN}^2 m_N, \qquad \left\langle \frac{1}{m_N}\right\rangle = \sum_N \frac{U_{eN}^2}{m_N}. \tag{10}$$

Here, the NMEs $M_\nu'^{0\nu}, M_N'^{0\nu}$ are derived from the NME $M'^{0\nu}$ in Eq. (3) in the following way:

$$M'^{0\nu}(m_N \to 0, g_A^{\rm eff}) = \frac{1}{m_p m_e} M_\nu'^{0\nu}(g_A^{\rm eff}), \tag{11}$$

$$M'^{0\nu}(m_N \to \infty, g_A^{\rm eff}) = \frac{1}{m_N^2} M_N'^{0\nu}(g_A^{\rm eff}). \tag{12}$$

The values of $M_\nu'^{0\nu}(g_A^{\rm eff})$ and $M_N'^{0\nu}(g_A^{\rm eff})$ calculated in the QRPA with partial restoration of isospin symmetry [24] for all the experimentally interesting isotopes are given in Table I (for more details of the formalism, see e.g., Refs. [21–23]). These NMEs can be used for the analysis of the light and the heavy Majorana exchange mechanisms of $0\nu\beta\beta$ decay on the basis of Eqs. (9).

What we would like to highlight here is that these limiting-case NMEs also allow one to approximate the NME or half-life for arbitrary m_N with the aid of a useful “interpolating formula” proposed in Ref. [33] and used in the literature (see e.g., Refs. [19,28]) in analysis of $0\nu\beta\beta$ decay. For the half-life, it reads

TABLE I. The values of the nuclear matrix elements for the light and heavy neutrino mass mechanisms defined in Eqs. (11) and (12) and the parameters $\langle p^2\rangle$ and $\mathcal{A}$ of the interpolating formula specified in Eqs. (13)–(15). The calculations have been carried out within the QRPA with partial restoration of isospin symmetry [24]. Two different types of NN potential (CD–Bonn and Argonne) as well as quenched ($g_A = 1.00$) and unquenched ($g_A = 1.269$) values of the nucleon axial-vector constant have been considered. The cases presented are a) Argonne potential, $g_A = 1.00$; b) Argonne, $g_A = 1.269$; c) CD–Bonn, $g_A = 1.00$; and d) CD–Bonn, $g_A = 1.269$.

	$M'^{0\nu}_{\nu}$				$M'^{0\nu}_{N}$				$\sqrt{\langle p^2\rangle}$ (MeV)				$\mathcal{A}$ (10^{-10} yrs^{-1})			
Nucleus	a	b	c	d	a	b	c	d	a	b	c	d	a	b	c	d
^{48}Ca	0.463	0.541	0.503	0.594	29.0	40.3	49.0	66.3	173.0	189.0	216.0	231.0	0.541	1.05	1.55	2.83
^{76}Ge	3.886	5.157	4.211	5.571	204.0	287.0	316.0	433.0	159.0	163.0	190.0	193.0	2.55	5.05	6.12	11.5
^{82}Se	3.460	4.642	3.746	5.018	186.0	262.0	287.0	394.0	161.0	165.0	192.0	194.0	9.12	18.1	21.7	40.9
^{96}Zr	2.154	2.717	2.341	2.957	132.0	184.0	202.0	276.0	171.0	180.0	203.0	212.0	9.30	18.1	21.8	40.7
^{100}Mo	4.185	5.402	4.525	5.850	244.0	342.0	371.0	508.0	167.0	174.0	198.0	204.0	24.6	48.3	56.8	107.
^{110}Pd	4.485	5.762	4.856	6.255	238.0	333.0	360.0	492.0	160.0	166.0	189.0	194.0	7.07	13.8	16.2	30.2
^{116}Cd	3.086	4.040	3.308	4.343	150.0	209.0	222.0	302.0	153.0	157.0	179.0	183.0	9.74	18.9	21.3	39.5
^{124}Sn	2.797	2.558	3.079	2.913	146.0	184.0	224.0	279.0	158.0	186.0	187.0	214.0	5.00	7.94	11.8	18.2
^{128}Te	3.445	4.563	3.828	5.084	215.0	302.0	331.0	454.0	173.0	178.0	204.0	207.0	0.705	1.39	1.67	3.14
^{130}Te	2.945	3.888	3.297	4.373	189.0	264.0	292.0	400.0	175.0	180.0	206.0	209.0	13.2	25.7	31.4	59.0
^{136}Xe	1.643	2.177	1.847	2.460	108.0	152.0	166.0	228.0	178.0	183.0	208.0	211.0	4.41	8.74	10.4	19.7

$$[T^{0\nu}_{1/2}]^{-1} = \mathcal{A}\cdot\left|m_p \sum\nolimits_N U^2_{eN}\frac{m_N}{\langle p^2\rangle + m_N^2}\right|^2, \qquad (13)$$

where

$$\mathcal{A} = G^{0\nu} g_A^4 |M'^{0\nu}_N(g_A^{\rm eff})|^2, \qquad (14)$$

$$\langle p^2\rangle = m_p m_e \left|\frac{M'^{0\nu}_N(g_A^{\rm eff})}{M'^{0\nu}_\nu(g_A^{\rm eff})}\right|^2, \qquad (15)$$

with the values of the matrix elements $M'^{0\nu}_\nu, M'^{0\nu}_N$ and parameters $\langle p^2\rangle$ and $\mathcal{A}$ given for various isotopes in Table I. To estimate the accuracy of the approximate formula (13), we compare it with the "exact" QRPA results in Fig. 1 for ^{76}Ge and ^{136}Xe, where the dotted curves correspond to the interpolating formula (13). As seen, it is a rather good approximation of the exact QRPA result except for the transition region in which the accuracy is about 20%–25%.

The clear advantage of the formula (13) is that it shows explicitly the m_N dependence of the $0\nu\beta\beta$ amplitude or the half-life. Therefore, it can be conveniently used for an analysis of any contents of the neutrino sector without engaging the sophisticated machinery of the nuclear structure calculations. Also, any upgrade of nuclear structure approaches typically bringing out asymptotical NMEs for $m_N \ll p_F$ and $m_N \gg p_F$ allows one to immediately reconstruct with a good accuracy updated NMEs for arbitrary m_N.

For completeness, let us give the $0\nu\beta\beta$-decay half-life formula for a generic neutrino spectrum, which incorporates a popular scenario neutrino Minimal Standard Model (νMSM) [34,35], offering a solution of the dark matter (DM) and baryon asymmetry (BAU) problems via massive Majorana neutrinos. In Refs. [36], $0\nu\beta\beta$ decay has been considered within the νMSM employing certain approximations in order to estimate $0\nu\beta\beta$-decay half-life. We note that our Eq. (13) offers a suitable and systematic tool for this purpose especially when both small and large values of m_N are involved.

Let the neutrino spectrum contain (i) three light neutrinos $\nu_{k=1,2,3}$ with the masses $m_{\nu(k)} \ll p_F \sim 200$ MeV dominated by $\nu_{e,\mu,\tau}$, (ii) a number of the DM candidate neutrinos $\nu_i^{\rm DM}$ with the masses $m_i^{\rm DM}$ at the keV scale, (iii) a number of heavy neutrinos N with the masses $m_N \gg p_F$, plus (iv) several intermediate mass m_h neutrinos h among which there could be a pair highly degenerate in mass needed for the generation of the BAU via leptogenesis [35]. In this case, the interpolating formula (13) allows us to write down for the half-life of any $0\nu\beta\beta$-decaying isotope

$$[T^{0\nu}_{1/2}]^{-1} = \mathcal{A}\left|\frac{m_p}{\langle p^2\rangle}\sum_{k=1}^{3} U^2_{ek} m_k + \frac{m_p}{\langle p^2\rangle}\sum_i (U^{\rm DM}_{ei})^2 m_i^{\rm DM} + m_p \sum_N \frac{U^2_{eN}}{m_N} + m_p\sum_h \frac{U^2_{eh} m_h}{\langle p^2\rangle + m_h^2}\right|^2. \qquad (16)$$

Here, because of typically very small mixing between the light and massive neutrino mass eigensates $|U^{\rm DM}_{ei}|, |U_{eN}|$, and $|U_{eh}| \ll |U_{ek}|$, the mixing matrix of the light neutrinos ν_k to a good accuracy can be identified with the element of the Pontecorvo-Maki-Nakagawa-Sakata (PMNS) mixing matrix $U_{ek} \approx U^{\rm PMNS}_{ek}$.

Finally, the following observation might be of interest. Note that the parameter $\langle p^2\rangle$ with the typical value $\sim(200\ {\rm MeV})^2$ can be interpreted as the mean Fermi momentum of nucleons p_F in a nucleus. This is suggested by the structure of the NME in Eq. (3). In fact, we can schematically write for the m_N dependence

$$M'^{0\nu}(m_N) \simeq {\rm const}\cdot \int_0^\infty \frac{h(p^2)p^2 dp}{\sqrt{p^2+m_N^2}(\sqrt{p^2+m_N^2}+\bar{E}_n)} \simeq {\rm const}\cdot\frac{1}{p^2+m_N^2} \equiv {\rm const}\cdot \frac{1}{\langle p^2\rangle + m_N^2}. \qquad (17)$$

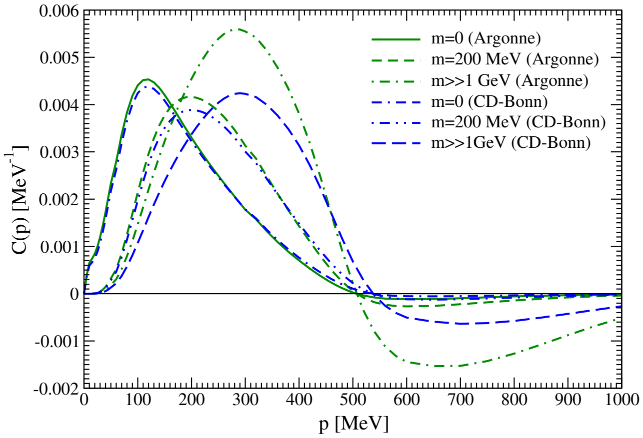

FIG. 2 (color online). The normalized momentum transfer p distribution $C(p)$ [24] of the virtual neutrino characterizing its contribution to the nuclear matrix element (3) in the function of p.

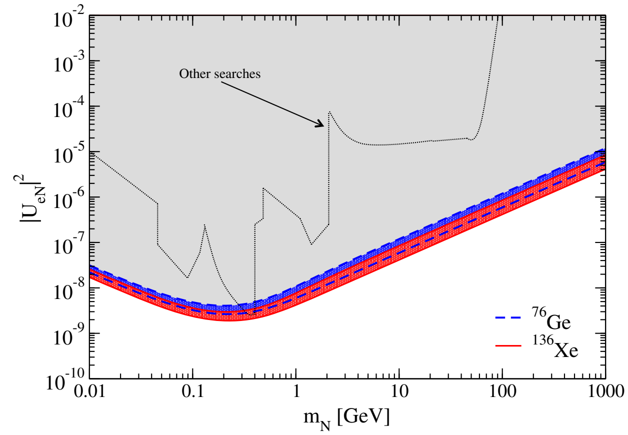

FIG. 3 (color online). Exclusion plots in the $|U_{eN}|^2 - m_N$ plane. The band restricted by blue dashed lines (red solid lines) is the lower limit from the experimental searches for $0\nu\beta\beta$ decay of ^{76}Ge (^{136}Ge). The weakest (strongest) limit is obtained for $M^{0\nu}(m_N)$ calculated with Argonne potential (CD–Bonn potential) and assuming $g_A = 1.00$ ($g_A = 1.269$). The thin dotted line other searches shows a region excluded from the various laboratory searches for massive neutrinos [18,20].

Here, $\bar{E}_n = E_n - (E_I - E_F)/2 \sim 10$ MeV is a small value in comparison with the so-defined mean neutrino momentum $\overline{p^2}$, taking into account the smearing effect of the nucleon form factors and the nuclear wave function codified in the $h(p^2)$ factor (for definitions, see Ref. [22]). In the last step in Eq. (17), we identified $\overline{p^2}$ with the parameter $\langle p^2\rangle$ in Eq. (13) as suggested by the comparison of Eq. (13) with Eq. (17). Kinematically, the mean momentum transfer such us $\sqrt{\langle p^2\rangle}$ is expected to be of the order of the mean nucleon Fermi momentum p_F in a nucleus.

Although $\langle p^2\rangle$ is just a parameter of the parametrization (13) tabulated in Table I, its rather small variation over the isotopes supports the above physical interpretation. On top of that, we show in Fig. 2 the normalized momentum transfer distribution $C(p)$ defined in Ref. [24]. It characterizes the contribution of the momentum p to the NME for several values of m_N and two options for the NN potential. As seen from Fig. 2 for the intermediate mass $m_N = 200$ MeV corresponding to the transition region of the interpolating formula in Eq. (13), the NME is dominated by the mean value of the virtual neutrino momentum $p \approx 200$ MeV. This fact again indicates that the parameter $\sqrt{\langle p^2\rangle}$ is correlated with the mean momentum transfer and, consequently, with p_F. The above-given interpretation could be useful for gross estimates analyzing systems for which the NMEs are unavailable.

IV. EXPERIMENTAL LIMITS

Having the nuclear matrix element $M'^{0\nu}(m_N)$ calculated, we can derive the $0\nu\beta\beta$-decay limits on the mass m_N of the N neutrino and its mixing U_{eN} with the ν_e neutrino weak eigenstate. Here, we assume no significant cancellation between different terms in Eq. (2) or (13). In other words, we consider only one term in Eqs. (2) and (13). Applying the presently best lower bounds on the $0\nu\beta\beta$-decay half-life of ^{76}Ge (combined GERDA + Heidelberg − Moscow) [26] and ^{136}Xe (combined EXO + KamlandZEN) [27],

$$T^{0\nu}_{1/2}(^{76}\mathrm{Ge}) \geq T^{0\nu-\mathrm{exp}}_{1/2}(^{76}\mathrm{Ge}) = 3.0 10^{25}\ \mathrm{yrs},$$
$$T^{0\nu}_{1/2}(^{136}\mathrm{Xe}) \geq T^{0\nu-\mathrm{exp}}_{1/2}(^{136}\mathrm{Xe}) = 3.4 10^{25}\ \mathrm{yrs}, \qquad (18)$$

we derived from Eq. (2) the $|U_{eN}|^2 - m_N$ exclusion plot shown in Fig. 3. Alternatively, as we demonstrated in Sec. III, the same could be done on the basis of the interpolating formula in Eq. (13) without visible changes in Fig. 3.

In Fig. 3, we also show typical domains excluded by some other experiments summarized in Refs. [18,20]. These domains are just indicative because most of the previous bounds were obtained for some fixed values of m_N. For convenience, we interpolated this set of experimental points by continuous curves in different intervals of m_N. As seen from Fig. 3, the $0\nu\beta\beta$-decay limits exclude the parts of the $|U_{eN}|^2 - m_N$ parameter space previously unconstrained by the laboratory experiments except for a very small interval $m_N = 300$–400 MeV.[1] However, the following comment here is in order. The constraints listed in Refs. [20] are based on the searches for peaks in

[1]Note that our exclusion plot in Fig. 3 is given for $m_N \geq 10$ MeV, where other constraints [18,20] for comparatively heavy N are located. Obviously, it can be extrapolated both in $m_N \to 0$ and $m_N \to \infty$ directions since our approach is valid for arbitrary m_N. Outside the region of m_N in Fig. 3, our curve is given with a good accuracy by the second and the third terms of Eq. (16).

differential rates of various processes and the direct production of N states followed by their decays in a detector. In Refs. [19,37], it was pointed out that in this case the results of data analysis depend on the total decay width of N, including the neutral current decay channels. The latter have not been properly taken into account in the derivation of the mentioned experimental constraints. However, the neutral current N-decay channels introduce the dependence of the final results on all the mixing matrix elements U_{eN}, $U_{\mu N}$, and $U_{\tau N}$. In this situation, one cannot extract individual limits for these matrix elements without some additional assumptions, introducing a significant uncertainty. In contrast, our $0\nu\beta\beta$-decay limits involve only the U_{eN} mixing matrix element and therefore are free of the mentioned uncertainty. This is because in $0\nu\beta\beta$ decay intermediate Majorana neutrinos are always off-mass-shell states and their decay widths are irrelevant. On the other hand, the above-derived $0\nu\beta\beta$-decay constraints may be significantly weakened in the presence of the CP Majorana phases $\alpha^{CP} \neq 2\pi n$, for an integer n. This is because, in that case, in Eqs. (2), (13), and (16), a cancellation between different terms may happen.

V. SUMMARY

We updated the $0\nu\beta\beta$-decay limits in the plane $|U_{eN}|^2 - m_N$ for the updated nuclear matrix elements [24] and experimental data (18). Our limits are shown in Fig. 3. We studied some uncertainties endemic to the nuclear structure calculations in general and for the QRPA in particular. These are the choice of the NN-potential and the value of the nucleon axial-vector coupling $g_A^{\rm eff}$ in nuclear matter. In Fig. 3, we compared the $0\nu\beta\beta$-decay limits with the corresponding limits from other searches and showed that the former confidently override the latter for all m_N values except for a narrow interval around ~300 MeV at which certain improvement of the $0\nu\beta\beta$-decay limits is needed. We also commented on the reliability of both the experimental results shown in Fig. 3 as “other searches” and the $0\nu\beta\beta$-decay limits themselves disclosing some assumptions incorporated in their derivation.

We analyzed the interpolating formula, Eq. (13), from the viewpoint of its accuracy and usefulness in phenomenological analysis of neutrino models in the part of their predictions for $0\nu\beta\beta$ decay. This formula allows one to easily update $0\nu\beta\beta$-decay limits for $|U_{eN}|^2 - m_N$ once either new experimental data for the $0\nu\beta\beta$-decay half-life or updated NMEs for the light and heavy Majorana exchange mechanisms are released. As an application of this formula, we gave an approximate representation of the $0\nu\beta\beta$-decay half-life in Eq. (16) for the neutrino spectrum of the presently popular νMSM scenario [34,35].

ACKNOWLEDGMENTS

F. Š. acknowledges the support by the VEGA Grant agency of the Slovak Republic under Contract No. 1/0876/12 and by the Ministry of Education, Youth and Sports of the Czech Republic under Contract No. LM2011027. The work was partially supported by the PIIC fellowship (M. G.) from Universidad Técnica Federico Santa María (UTFSM) and the research grant (S. K.) from the UTFSM.

[1] J. Schechter and J. Valle, Phys. Rev. D **25**, 2951 (1982).
[2] M. Hirsch, S. Kovalenko, and I. Schmidt, Phys. Lett. B **642**, 106 (2006).
[3] P. Minkowski, Phys. Lett. **67B**, 421 (1977); T. Yanagida, in *Proceedings of Workshop on Grand Unified Theory and Baryon Number of the Universe, Tsukuba, Japan, 1979*, edited by O. Sawada and A. Sugamoto (KEK, Japan, 1979); M. Gell-Mann, P. Ramond, and R. Slansky, Report No. CALT-68-709; *Supergravity* edited by (North Holland, Amsterdam, 1979); S. L. Glashow, *Quarks and Leptons*, Cargese, edited by M. Levy *et al.* (Plenum, New York, 1980), p. 707; R. N. Mohapatra and G. Senjanovic, Phys. Rev. Lett. **44**, 912 (1980).
[4] M. Fukugita and T. Yanagida, Phys. Lett. B **174**, 45 (1986).
[5] W.-Y. Keung and G. Senjanovic, Phys. Rev. Lett. **50**, 1427 (1983).
[6] B. Allanach, C. Kom, and H. Päs, Phys. Rev. Lett. **103**, 091801 (2009).
[7] V. Tello, M. Nemevsek, F. Nesti, G. Senjanovic, and F. Vissani, Phys. Rev. Lett. **106**, 151801 (2011).
[8] M. Nemevšek, F. Nesti, G. Senjanovic, and Y. Zhang, Phys. Rev. D **83**, 115014 (2011).
[9] J. Helo, M. Hirsch, S. Kovalenko, and H. Päs, Phys. Rev. D **88**, 011901 (2013).
[10] J. Helo, M. Hirsch, H. Päs, and S. Kovalenko, Phys. Rev. D **88**, 073011 (2013).
[11] J. Helo, M. Hirsch, and S. Kovalenko, Phys. Rev. D **89**, 073005 (2014).
[12] J. Vergados, H. Ejiri, and F. Šimkovic, Rept. Prog. Phys. **75**, 106301 (2012).
[13] F. F. Deppisch, M. Hirsch, and H. Päs, J. Phys. G **39**, 124007 (2012).
[14] W. Rodejohann, Int. J. Mod. Phys. E **20**, 1833 (2011).
[15] P. Bamert, C. P. Burgess, and R. N. Mohapatra, Nucl. Phys. **B438**, 3 (1995).
[16] P. Benes, A. Faessler, F. Šimkovic, and S. Kovalenko, Phys. Rev. D **71**, 077901 (2005).
[17] K. N. Abazajian *et al.*, arXiv:1204.5379.
[18] A. Atre, T. Han, S. Pascoli, and B. Zhang, J. High Energy Phys. 05 (2009) 030.

[19] J. C. Helo, S. Kovalenko, and I. Schmidt, Nucl. Phys. **B853**, 80 (2011).

[20] J. Beringer *et al.* (Particle Data Group), Phys. Rev. D **86**, 010001 (2012).

[21] V. A. Rodin, A. Faessler, F. Šimkovic, and P. Vogel, Phys. Rev. C **68**, 044302 (2003); Nucl. Phys. **A766**, 107 (2007); **A793**, 213 (2007).

[22] F. Šimkovic, A. Faessler, V. A. Rodin, P. Vogel, and J. Engel, Phys. Rev. C **77**, 045503 (2008).

[23] F. Šimkovic, A. Faessler, H. Muther, V. Rodin, and M. Stauf, Phys. Rev. C **79**, 055501 (2009).

[24] F. Šimkovic, V. Rodin, A. Faessler, and P. Vogel, Phys. Rev. C **87**, 045501 (2013).

[25] M. Blennow, E. Fernandez-Martinez, J. Lopez-Pavon, and J. Menendez, J. High Energy Phys. 07 (2010) 096.

[26] M. Agostini *et al.* (GERDA Collaboration), Phys. Rev. Lett. **111**, 122503 (2013).

[27] A. Gando *et al.* (KamLAND-Zen Collaboration), Phys. Rev. Lett. **110**, 062502 (2013).

[28] M. Mitra, G. Senjanovic, and F. Vissani, Nucl. Phys. **B856**, 26 (2012); A. Abada, V. De Romeri, and A. M. Teixeira, J. High Energy Phys. 09 (2014) 074.

[29] J. Kotila and F. Iachello, Phys. Rev. C **85**, 034316 (2012).

[30] B. H. Wildenthal, M. S. Curtin, and B. A. Brown, Phys. Rev. C **28**, 1343 (1983); D. H. Wilkinson, *Physics with Heavy Ions and Mesons*, edited by R. Balian, M. Rho, and G. Ripka (North Holland, Amsterdam, 1978); B. Buck and S. M. Perez, Phys. Rev. Lett. **50**, 1975 (1983); K. Langanke, D. J. Dean, P. B. Radha, Y. Alhassid, and S. E. Koonin, arXiv:nucl-th/9504019.

[31] A. Faessler, G. L. Fogli, V. Rodin, E. Lisi, A. M. Rotunno, and F. Šimkovic, J. Phys. G **35**, 075104 (2008).

[32] J. Barea, J. Kotila, and F. Iachello, Phys. Rev. C **87**, 014315 (2013).

[33] S. Kovalenko, Z. Lu, and I. Schmidt, Phys. Rev. D **80**, 073014 (2009).

[34] T. Asaka and M. Shaposhnikov, Phys. Lett. B **620**, 17 (2005).

[35] T. Asaka, S. Blanchet, and M. Shaposhnikov, Phys. Lett. B **631**, 151 (2005).

[36] F. L. Bezrukov, Phys. Rev. D **72**, 071303 (2005); T. Asaka, S. Eijima, and H. Ishida, J. High Energy Phys. 04 (2011) 011; A. Merle and V. Niro, Phys. Rev. D **88**, 113004 (2013).

[37] C. Dib, V. Gribanov, S. Kovalenko, and I. Schmidt, Phys. Lett. B **493**, 82 (2000); V. Gribanov, S. Kovalenko, and I. Schmidt, Nucl. Phys. **B607**, 355 (2001).